Formation of Trinuclear Complexes by Addition of Mercury(II) Halides and Gold(I) Halides to $Pt_2(\mu\text{-dpm})_2(CN)_2$

Dawn V. Toronto and Alan L. Balch*

Department of Chemistry, University of California, Davis, California 95616

Received July 14, 1994[⊗]

Treatment of $Pt_2(\mu\text{-dpm})_2(CN)_2$ (dpm is bis(diphenylphosphino)methane) with 1 equiv of mercury(II) iodide in a dichloromethane/methanol solution yields orange $(NC)_2Pt_2(\mu\text{-I})(\mu\text{-HgI})(\mu\text{-dpm})_2\cdot CH_2Cl_2\cdot 1.5H_2O$, **4**, which crystallizes in the triclinic space group with $a = 15.311(3)$ Å, $b = 16.132(5)$ Å, and $c = 24.911(6)$ Å at 130 K with $Z = 4$. Refinement of 11040 reflections and 416 parameters gave $R = 0.084$ and $R_w = 0.117$. There are two, nearly identical, molecules in the asymmetric unit. Each consists of a doubly bridged A-frame with $[HgI]^+$ and I^- fragments at the bridging sites. The Pt−Hg bond lengths for molecule A are 2.729(2) and 2.700(2) Å and for molecule B are 2.725(2) and 2.700(2) Å. The platinum−platinum bond is retained, Pt−Pt distance 2.823(2) Å (molecule B, 2.819(2) Å). Treatment of $Pt_2(\mu\text{-dpm})_2(CN)_2$ with 1 equiv of mercury(II) bromide, under similar reaction conditions, yields $(NC)_2Pt_2(\mu\text{-Br})(\mu\text{-HgBr})(\mu\text{-dpm})_2$, **5**. Treatment of $Pt_2(\mu\text{-dpm})_2(CN)_2$ with 1 equiv of Me_2SAuCl in dichloromethane yields yellow $(NC)_2Pt_2(\mu\text{-AuCl})(\mu\text{-dpm})_2\cdot CH_2Cl_2$, **6**, which crystallizes in the tetragonal space group $P4_3$ with $a = 20.933(5)$ Å and $c = 14.381(6)$ Å at 130 K with $Z = 4$. Refinement of 3473 reflections and 300 parameters gave $R = 0.059$ and $R_w = 0.081$. The structure consists of two Pt(CN) groups spanned by two mutually perpendicular trans dpm ligands and bridged symmetrically by a AuCl fragment to form an A-frame. The Pt−Pt bond length (2.821(2) Å) and Pt−Au bond lengths (2.633(2) and 2.648(2) Å) are consistent with the presence of a two-electron, three-center bond between the three metal centers.

Introduction

The reactivity of the metal−metal bond of $Pt_2(\mu\text{-dpm})_2X_2$ and $Pd_2(\mu\text{-dpm})_2X_2$, **1** (dpm is bis(diphenylphosphino)methane),

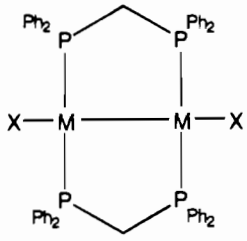

1

M = Pt or Pd, X = halide or pseudo-halide

toward insertion reactions of small molecules and transition metal fragments to produce molecular A-frames has been well developed.[1−4] The original prediction by Hoffman and Hoffmann[5] that stable trimetallic A-frame clusters would be formed by the insertion of an ML_2 d^{10} or ML_4 d^8 metal fragment into **1** was based on the isolobal relationship with the known insertion of the methylene group.[6,7] Since then, both HgX_2 and AuX have been shown to insert directly into the Pt−Pt bond of **1** to produce the stable trimetallic clusters $Pt_2(\mu\text{-HgCl}_2)(\mu\text{-dpm})_2Cl_2$, **2**,[8] and $Pt_2(\mu\text{-AuCl})(\mu\text{-dpm})_2Cl_2$, **3**.[9] Attempts at inserting

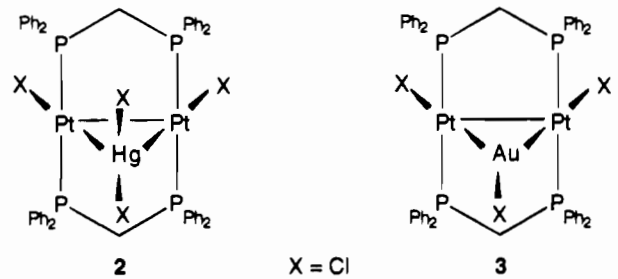

2 X = Cl **3**

other metals has proved unsuccessful; $SnCl_2$ does not add to either the Pt−Pt or Pd−Pd bonds but inserts into the M−Cl bond to give $M_2Cl(SnCl_3)(\mu\text{-dpm})_2$ (M = Pd or Pt),[10,11] and carbonylmetalates such as $[Fe(CO)_4]^{2-}$ produce *triangulo*-Pt_2Fe complexes in which the $\{Pt_2(\mu\text{-dpm})_2\}$ skeleton is disrupted, and an Fe−P bond is formed.[12] Additionally, insertion of Hg(II) or Au(I) fails when palladium is substituted for platinum (*i.e.*, in $Pd_2(\mu\text{-dpm})_2Cl_2$) or when the parent dimer is a mixed-metal complex $(PdPt(\mu\text{-dpm})_2Cl_2)$.[9]

Hoffman and Hoffmann originally predicted the formation of stable A-frame clusters such as **2** and **3** on the basis of the isolobal relationship of the transition metal fragment ML_2 (d^{10}) with H^+.[5] This implies that the important bonding interaction

[⊗] Abstract published in *Advance ACS Abstracts,* November 15, 1994.

(1) Balch, A. L. In *Homogeneous Catalysis with Metal Phosphine Complexes*; Pignolet, L. H., Ed.; Plenum Press: New York, 1983; p 167.
(2) Puddephatt, R. J. *Chem. Soc. Rev.* **1983**, *12*, 99.
(3) Chaudret, B.; Delavaux, B.; Poilblanc, R. *Coord. Chem. Rev.* **1988**, *86*, 191.
(4) Anderson, G. K. *Adv. Organomet. Chem.* **1993**, *35*, 1.
(5) Hoffman, R.; Hoffmann, D. M. *Inorg. Chem.* **1981**, *20*, 3543.
(6) Brown, M. P.; Fisher, J. R.; Puddephatt, R. J.; Seddon, K. R. *Inorg. Chem.* **1979**, *18*, 2808.
(7) Balch, A. L.; Hunt, C. T.; Lee, C.-L.; Olmstead, M. M.; Farr, J. P. *J. Am. Chem. Soc.* **1981**, *103*, 3764.
(8) Sharp, P. R. *Inorg. Chem.* **1986**, *25*, 4185.
(9) Puddephatt, R. J.; Arsenault, G. J. *Can. J. Chem.* **1989**, *67*, 1800.
(10) Olmstead, M. M.; Benner, L. S.; Hope, H.; Balch, A. L. *Inorg. Chim. Acta* **1979**, *32*, 193.
(11) Grossel, M. C.; Moulding, R. P.; Seddon, K. R. *Inorg. Chim. Acta* **1982**, *64*, L275.
(12) Grossel, M. C.; Moulding, R. P.; Seddon, K. R. *J. Organomet. Chem.* **1983**, *253*, C50.

0020-1669/94/1333-6132$04.50/0

in these clusters is the orbital of a_1 symmetry, with very little contribution from the b_1 orbital on the added fragment.

Sharp also reached similar conclusions for **2** on the basis of ^{31}P NMR and structural data.[8] The addition of the third metal to the parent dimer changes the electronic structure and lowers the energy of the metal-centered transitions ($\sigma_{a_1} \rightarrow \sigma^*_{b_1}$). This can be seen by visually comparing $Pt_2(\mu\text{-dpm})_2Cl_2$, **1** (M = Pt, X = Cl), which is yellow, to $Pt_2(\mu\text{-HgCl}_2)(\mu\text{-dpm})_2Cl_2$, **2**, and $Pt_2(\mu\text{-AuCl})(\mu\text{-dpm})_2Cl_2$, **3**, which are orange. On the basis of these observations, we began to study the electronic structure and spectroscopic properties of **2** and **3**. We recently reported absorption spectra and photoluminescence from these electron deficient A-frame complexes and used SCF−Xα−SW calculations to describe the differences which occur between the mercury and gold adduct.[13] Our calculations are in agreement with those of Hoffman and Hoffmann[5] and reveal that the primary differences in the two clusters result from the lower energy of the orbitals on mercury than on gold. For both clusters the addition of the third metal center leads to a stabilization of both the LUMO (σ^*, b_1) and HOMO (σ, a_1) and a narrowing of the HOMO−LUMO gap from the parent dimer. For **2** the HOMO remains the σ orbital, but the LUMO becomes largely Hg-s with the σ^* slightly higher in energy. In **3**, the HOMO changes and becomes mainly π^* d_{xz} while the LUMO remains σ^*. The calculations complement the spectral data. The absorption spectra of the two adducts are red shifted from the parent and differ in detail, but the energies of the lowest excited states are similar.

In our continued interest in the electronic structure of these molecular A-frames, we extended these studies to A-frame derivatives of $Pt_2(\mu\text{-dpm})_2(CN)_2$. Replacement of the π-donor halide ligands by the π-acceptor cyanide ligands should change the reactivity at the metal−metal bond and lead to different structural features and electronic properties. Here we describe the formation of three new molecular A-frames by addition of the transition metal fragments HgX_2 and AuX to $Pt_2(\mu\text{-dpm})_2(CN)_2$.

Results

Synthetic Studies. Addition of mercury(II) bromide or mercury(II) iodide to $Pt_2(\mu\text{-dpm})_2(CN)_2$ leads to the formation of doubly bridged molecular A-frames **4** and **5** (eq 1). Reaction of methanolic mercury(II) iodide with a dichloromethane solution of $Pt_2(\mu\text{-dpm})_2(CN)_2$ results in a color change from pale yellow to orange. Concentration of the solution results in the formation of orange crystals of $(NC)_2Pt_2(\mu\text{-I})(\mu\text{-HgI})(\mu\text{-dpm})_2$, **4**, whose structure has been determined crystallographically (*vide infra*). The bromo analog can be synthesized by substituting mercury(II) bromide for mercury(II) iodide. From the yellow solution, the dark yellow crystalline compound $(NC)_2Pt_2(\mu\text{-Br})(\mu\text{-HgBr})(\mu\text{-dpm})_2$, **5**, can be isolated. The spectroscopic data and electronic data confirm that the structure of **5** is similar to that of **4**. The electronic absorption spectra and the lack of emission for both **4** and **5** differentiate them from the previously reported A-frames. Relevant data are shown

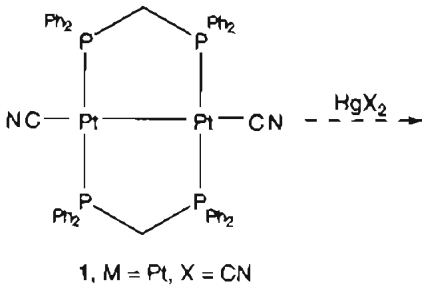

1, M = Pt, X = CN

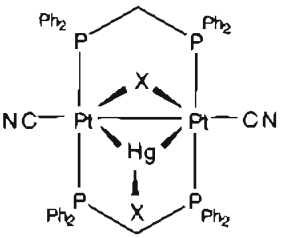

(1)

4, I
5, Br

in Figure 1. The electronic absorption spectrum of a dichloromethane solution of **4** (trace A) shows one low energy transition at λ_{max} (nm (ϵ, M^{-1} cm^{-1})) 400 (11 000) with a shoulder at 450 (3800). The absorption spectrum of the bromo analog (trace B) exhibits similar features with a slight shift to higher energies (372 (5900), 430 (1300)). In contrast, the absorption spectra of $Pt_2(\mu\text{-HgCl}_2)(\mu\text{-dpm})_2Cl_2$ and $Pt_2(\mu\text{-HgBr}_2)(\mu\text{-dpm})_2Br_2$ show three low energy transitions: 382 (2300), 428 (2100), 480 (1500) and 398 (3500), 428 (2400), 486 (1900), respectively. Previous work has shown that these transitions are metal centered.[13] In addition, as shown in trace C of Figure 1, **2** (X = Br) shows intense, red luminescence when frozen at 77 K. However, no emission is observable at room temperature.

When the same synthetic technique shown in eq 1 is used to form the gold chloride adduct from $Pt_2(\mu\text{-dpm})_2(CN)_2$, the conventional singly bridged A-frame complex, **6**, is isolated (eq 2). Addition of Me_2SAuCl to a dichloromethane solution of

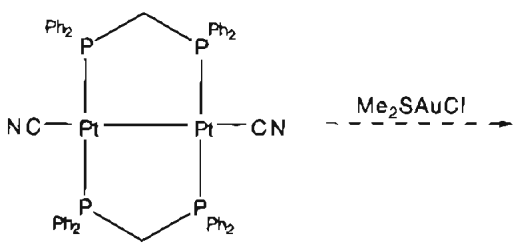

1

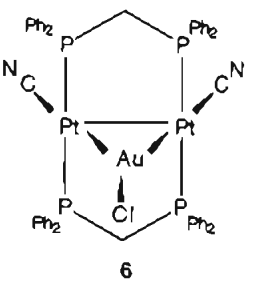

(2)

6

$Pt_2(\mu\text{-dpm})_2(CN)_2$ turns the pale, yellow solution bright yellow. Concentration of the solution and addition of diethyl ether yield yellow crystals of $(NC)_2Pt_2(\mu\text{-AuCl})(\mu\text{-dpm})_2$, **6**. Because neither the spectroscopic data nor the electronic absorption data

(13) Toronto, D. V.; Tinti, D.; Balch, A. L. *Inorg. Chem.* **1994**, *33*, 2507.

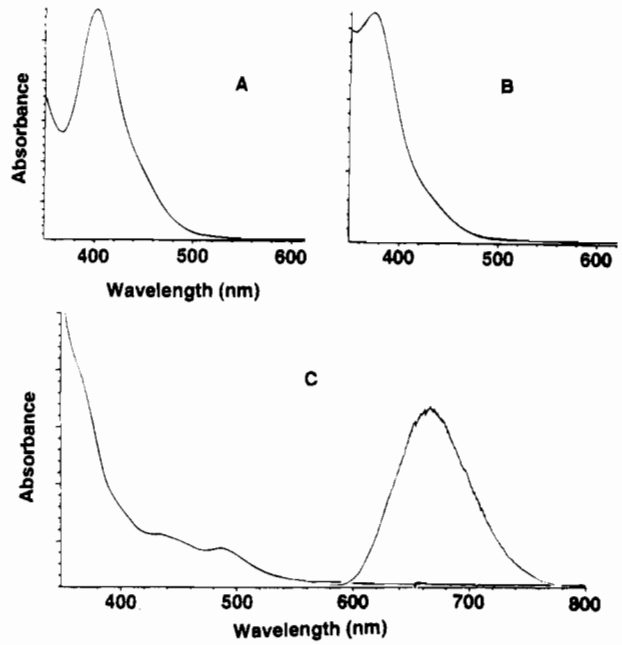

Figure 1. Electronic absorption spectra of dichloromethane solutions of (A), $Pt_2(\mu\text{-I})(\mu\text{-HgI})(\mu\text{-dpm})_2(CN)_2$ (**4**), and (B), $Pt_2(\mu\text{-Br})(\mu\text{-HgBr})(\mu\text{-dpm})_2(CN)_2$ (**5**). No emission could be observed for **4** and **5**. Trace C: electronic absorption of a dichloromethane solution of $Pt_2(\mu\text{-HgBr}_2)(\mu\text{-dpm})_2Br_2$. The emission spectrum is shown to the right.

could confirm whether this was a singly or doubly bridged A-frame, X-ray crystallographic studies were performed.

Infrared spectral parameters for **4**–**6** are given in the Experimental Section. All complexes show only terminal cyanide stretching vibrations in their infrared spectra. NMR spectral data are collected in Table 1 along with the $^{31}P\{^1H\}$ chemical shifts of the parent compound $Pt_2(\mu\text{-dpm})_2(CN)_2$. The $^{31}P\{^1H\}$ NMR spectra for **4** and **5** reflect the presence of six different isotopomers. The 33.8% natural abundance of ^{195}Pt ($I = {}^1/_2$) and the 17% natural abundance of ^{199}Hg ($I = {}^1/_2$) result in the following nuclear spin systems: (I) Pt_2P_4Hg, AA′A″A‴; (II) $^{195}PtPtP_4Hg$, AA′A″A‴X; (III) $^{195}Pt^{195}PtP_4Hg$, AA′A″A‴XX′; (IV) $Pt_2P_4{}^{199}Hg$, AA′A″A‴Y; (V) $^{195}PtPtP_4{}^{199}Hg$, AA′A″A‴XY; (VI) $^{195}Pt^{195}PtP_4{}^{199}Hg$, AA′A″A‴XX′Y. The complexity of the spectra is simplified by the lack of coupling seen between phosphorus and mercury and the superposition of chemical shifts of the various isotopomers. The 64.3 MHz ^{195}Pt NMR spectrum for **4** consists of a single triplet, $\delta = -5096$ ppm (referenced to $K_2Pt_2Cl_4/D_2O$), with $^1J(Pt,P) = 2165$ Hz; Pt–Hg coupling could not be observed. The ^1H NMR spectrum, in deuterated chloroform, shows an AB pattern for the dpm methylene protons due to the asymmetry about the platinum–platinum bond. In addition to the AB coupling, coupling to ^{31}P and ^{195}Pt can be observed. Spectral analysis yields very similar coupling constants, and these constants are given in Table 1.

In attempts to add an additional iodide to the mercury iodide fragment to produce $[(NC)_2Pt_2(\mu\text{-I})(\mu\text{-HgI}_2)(\mu\text{-dpm})_2]^-$, the reactivity of $(NC)_2Pt_2(\mu\text{-I})(\mu\text{-HgI})(\mu\text{-dpm})_2$, **4**, with excess iodide was explored. Titration with monitoring by $^{31}P\{^1H\}$ NMR spectroscopy at −65 °C shows that, upon addition of 2 equiv of tetrabutylammonium iodide, partial decomposition of $(NC)_2Pt_2(\mu\text{-I})(\mu\text{-HgI})(\mu\text{-dpm})_2$ occurs to give the parent dimer $Pt_2(\mu\text{-dpm})_2(CN)_2$. This probably occurs with the formation of HgI_4^{2-}. When the sample is warmed to room temperature, the $^{31}P\{^1H\}$ NMR spectrum shows that both $(NC)_2Pt_2(\mu\text{-I})(\mu\text{-HgI})(\mu\text{-dpm})_2$ and $Pt_2(\mu\text{-dpm})_2(CN)_2$ are still present in solution.

The reactivity of $(NC)_2Pt_2(\mu\text{-AuCl})(\mu\text{-dpm})_2$ toward excess chloride ion was explored in an attempt to produce a doubly bridged species similar to $(NC)_2Pt_2(\mu\text{-I})(\mu\text{-HgI})(\mu\text{-dpm})_2$. Experimental conditions similar to those used in the titration of $(NC)_2Pt_2(\mu\text{-I})(\mu\text{-HgI})(\mu\text{-dpm})_2$ with iodide were employed. Complex **6** appears to be robust and shows no reactivity toward tetraphenylarsonium chloride.

Structure of $(NC)_2Pt_2(\mu\text{-I})(\mu\text{-HgI})(\mu\text{-dpm})_2\cdot 2CH_2Cl_2\cdot 1.5H_2O$, 4. This compound crystallizes with two independent molecules in the asymmetric unit with no crystallographically imposed symmetry. Selected atomic positional parameters for the two molecules are given in Table 2. A perspective view of molecule A is shown in Figure 2. Molecule B has a similar structure. A comparison of selected distances and angles for both molecules is presented in Table 3. This shows that there are only a few differences between the structures. Table 3 shows that the Pt–Hg bond lengths which characterize A and B are essentially identical. In molecule A the Pt–Hg distances (Pt(1)–Hg(1) 2.729(2), Pt(2)–Hg(1) 2.700(2) Å) are within experimental error of the Pt–Hg distances (Pt(3)–Hg(2) 2.725(2), Pt(4)–Hg(2) 2.700(2) Å) found in molecule B. The mercury atom is not positioned symmetrically between the two platinum atoms. Within each molecule, the internal Pt–Hg bond lengths vary by 0.029 and 0.025 Å for A and B, respectively. In contrast, the bridging iodine is more nearly centered between the two platinum atoms. A comparison of the Pt–I bond lengths (molecule A Pt(1)–I(2) 2.925(3) Å, Pt(2)–I(2) 2.907(2) Å; molecule B Pt(3)–I(102) 2.916(2) Å, Pt(4)–I(102) 2.911(3) Å) shows internal variations of only 0.018 and 0.005 Å for A and B, respectively.

In $Pt_2(\mu\text{-HgCl}_2)(\mu\text{-dpm})_2Cl_2$, **2**, there are also two molecules in the asymmetric unit and there are significant differences in the two Pt–Pt bond lengths (2.7119(8) and 2.7361(9) Å).[8] In $(NC)_2Pt_2(\mu\text{-I})(\mu\text{-HgI})(\mu\text{-dpm})_2$ the Pt–Pt bond lengths (molecule A Pt(1)–Pt(2) 2.823(2) Å; molecule B Pt(3)–Pt(4) 2.819(2) Å) are nearly identical. This is probably caused by the doubly bridging ligands which protect the metal–metal bond and constrain the distance. Because molecules A and B are essentially identical, all further reference to bond distances and angles will be made to molecule A, with the values for molecule B following in parentheses.

The overall structure of **4** is typical of the doubly-bridged A-frame class. The platinum atoms are bridged by a pair of trans dpm ligands, an iodide, and a $[HgI]^+$ fragment. The Pt–Hg bond lengths of 2.729(2) Å (2.725(2)) and 2.700(2) Å (2.700(2)) are consistent with the presence of bonding between these atoms. The platinum–platinum bond is retained as evidenced by the Pt(1)–Pt(2) distance of 2.823(2) Å (2.819(2)). The Pt–I distances of 2.925(3) Å (2.916(2)) and 2.907(2) Å (2.911(3)) show that the iodine is symmetrically placed between the two platinum atoms. A search in the Cambridge Crystallographic Database[14] shows that this complex is only the second iodine-bridged diplatinum species to be structurally characterized. The cation of $[Pt_2(\mu\text{-I})(\mu\text{-}o\text{-}C_6H_4PPh_2)_2(PPh_3)_2]I$, which contains two, approximately planar, Pt(II) atoms symmetrically bridged by two $o\text{-}C_6H_4PPh_2$ units and by an iodine atom, exhibits a much longer Pt–Pt distance (2.931(2) Å) and a shorter Pt–I distance (2.706(2) Å).[15] The large platinum–platinum distance in the cation is the result of a weak metal–metal bond formed between two Pt(II) metals. A formal metal–metal bond is not required for a 16-electron count around these

(14) Allen, F. H.; Davies, J. E.; Galloy, J. J.; Johnson, O.; Kennard, O.; Macral, C. F.; Mitchell, E. M.; Mitchell, G. F.; Smith, J. M.; Watson, D. G. *J. Chem. Inf. Comput. Sci.* **1991**, *31*, 187.
(15) Bennett, M. A.; Berry, D. E.; Bhargava, S. K.; Ditzel, E. J.; Robertson, G. B.; Willis, A. C. *J. Chem. Soc., Chem. Commun.* **1987**, 1613.

Table 1. Summary of NMR Spectral Parameters for **4**–**6** and $Pt_2(\mu\text{-dpm})_2(CN)_2$[a]

compd	$\delta(^{31}P\{^1H\})$, ppm	$^1J_{PtP}$, Hz	$^2J_{PtP}$, Hz	$^3J_{PP}$, Hz	$^3J_{PP}$, Hz	$\delta(^1H)(CH_2)$, ppm
4	−6.95	2168	−72	49	21	4.20, 5.10
5	8.60	2206	−77	40	13	5.50, 4.80
6	11.5	2316	−84	52	33	4.77, 5.39
$Pt_2(\mu\text{-dpm})_2(CN)_2$	−1.31	2809	−82	50	23	4.82

[a] Solvent or reference: ^{31}P, CD_2Cl_2; ^1H, CD_3Cl; ^{31}P, referenced to H_3PO_4.

Table 2. Atomic Coordinates ($\times 10^4$) and Equivalent Isotropic Displacement Coefficients ($Å^2 \times 10^3$) for $(NC)_2Pt_2(\mu\text{-I})(\mu\text{-HgI})(\mu\text{-dpm})_2{\cdot}CH_2Cl_2{\cdot}1.5H_2O$ (**4**)

	x	y	z	U[a]
Pt(1)	52031(7)	32438(7)	24642(5)	152(4)
Pt(2)	40276(7)	43800(7)	29615(5)	144(4)
Hg(1)	37963(7)	38631(8)	20014(5)	215(4)
I(1)	27890(13)	38889(15)	12232(9)	317(8)
I(2)	54631(12)	37334(12)	35216(8)	209(7)
P(1)	6145(5)	4285(5)	1964(3)	17(3)
P(2)	4853(5)	5534(5)	2536(3)	17(3)
P(3)	4295(5)	2122(5)	2850(3)	18(3)
P(4)	3051(5)	3357(5)	3433(3)	17(3)
N(1)	6507(17)	1945(18)	1941(12)	34(7)
N(2)	2647(17)	5570(18)	3456(12)	33(7)
C(1)	6052(16)	2390(17)	2153(12)	11(6)
C(2)	3154(18)	5169(18)	3279(12)	18(7)
C(15)	5999(17)	5286(18)	2255(13)	21(7)
C(40)	3493(15)	2329(15)	3453(11)	5(5)
Pt(3)	95038(7)	−6318(7)	29515(5)	142(4)
Pt(4)	85800(7)	−17591(7)	24555(5)	146(4)
Hg(2)	102178(7)	−11498(7)	19903(5)	209(4)
I(101)	116301(13)	−10994(15)	12186(9)	321(8)
I(102)	77755(12)	−12711(12)	35059(8)	217(7)
P(101)	8886(5)	515(5)	2518(1)	18(3)
P(102)	7882(5)	−722(5)	1961(3)	19(3)
P(103)	10218(5)	−1651(5)	3442(3)	20(3)
P(104)	9298(5)	−2887(5)	2843(3)	20(3)
N(101)	10680(18)	610(18)	3392(13)	39(7)
N(102)	7572(16)	−3073(17)	1936(11)	30(7)
C(101)	10236(20)	101(21)	3241(14)	32(8)
C(102)	7938(17)	−2592(18)	2127(12)	17(7)
C(115)	7920(17)	287(17)	2215(12)	14(6)
C(140)	9757(20)	−2705(20)	3446(14)	30(8)

[a] Equivalent isotropic U defined as one-third of the trace of the orthogonalized U_{ij} tensor. Coordinates for phenyl groups and solvate molecules are omitted; see supplementary material.

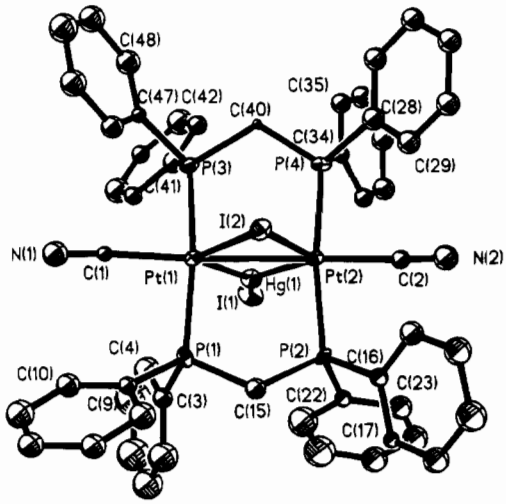

Figure 2. Perspective view of $Pt_2(\mu\text{-I})(\mu\text{-HgI})(\mu\text{-dpm})_2(CN)_2$ with 50% thermal ellipsoids.

platinum atoms. In **4** a formal platinum–platinum bond is required to give an even-electron count of either 16 or 18 electrons to the platinum atoms and is indicated by the short bond length. The Pt–I distances reported for the cation are shorter than the Pt–I distances of **4** due to the smaller atomic radius for platinum(II) atoms.

Table 3. Selected Bond Lengths (Å) and Angles (deg) for $(NC)_2Pt_2(\mu\text{-I})(\mu\text{-HgI})(\mu\text{-dpm})_2{\cdot}CH_2Cl_2{\cdot}1.5H_2O$ (**4**)

Bond Lengths

molecule A		molecule B	
Pt(1)–Hg(1)	2.729(2)	Pt(4)–Hg(2)	2.725(2)
Pt(2)–Hg(1)	2.700(2)	Pt(3)–Hg(2)	2.700(2)
Pt(1)–Pt(2)	2.823(2)	Pt(3)–Pt(4)	2.819(2)
Pt(1)–I(2)	2.925(3)	Pt(3)–I(102)	2.916(2)
Pt(2)–I(2)	2.907(2)	Pt(4)–I(102)	2.911(3)
Hg(1)–I(1)	2.656(3)	Hg(2)–I(101)	2.655(2)
Pt(2)–C(2)	1.98(3)	Pt(4)–C(102)	1.99(3)
Pt(1)–C(1)	2.03(3)	Pt(3)–C(101)	1.90(4)
Pt(1)–P(1)	2.323(7)	Pt(3)–P(101)	2.303(8)
Pt(1)–P(3)	2.305(7)	Pt(3)–P(103)	2.303(8)
Pt(2)–P(2)	2.303(7)	Pt(4)–P(102)	2.314(8)
Pt(2)–P(4)	2.310(7)	Pt(4)–P(104)	2.311(8)
C(1)–N(1)	1.12(4)	C(101)–N(101)	1.20(5)
C(2)–N(2)	1.08(4)	C(102)–N(102)	1.15(4)

Bond Angles

molecule A		molecule B	
Pt(1)–Hg(1)–Pt(2)	62.7(1)	Pt(3)–Hg(2)–Pt(4)	62.6(1)
Pt(1)–Hg(1)–I(1)	150.1(1)	Pt(3)–Hg(2)–I(101)	145.8(1)
Pt(2)–Hg(1)–I(1)	147.1(1)	Pt(4)–Hg(2)–I(101)	151.4(1)
Pt(2)–Pt(1)–Hg(1)	58.2(1)	Pt(4)–Pt(3)–Hg(2)	59.1(1)
Hg(1)–Pt(1)–I(2)	118.9(1)	Hg(2)–Pt(3)–I(102)	120.1(1)
Hg(1)–Pt(2)–I(2)	120.5(1)	Hg(2)–Pt(4)–I(102)	119.4(1)
Hg(1)–Pt(1)–P(1)	92.1(2)	Hg(2)–Pt(3)–P(101)	92.3(2)
Pt(2)–Pt(1)–P(3)	91.9(2)	Pt(4)–Pt(3)–P(103)	95.0(2)
I(2)–Pt(1)–P(3)	93.9(2)	I(102)–Pt(3)–P(103)	91.7(2)
Pt(2)–Pt(1)–C(1)	176.5(8)	Pt(4)–Pt(3)–C(101)	174.2(10)
I(2)–Pt(1)–C(1)	116.4(8)	I(102)–Pt(3)–C(101)	124.5(10)
I(2)–Pt(2)–P(2)	92.3(2)	I(102)–Pt(4)–P(102)	94.3(2)
Hg(1)–Pt(2)–P(4)	90.4(2)	Hg(2)–Pt(4)–P(104)	86.5(2)
P(2)–Pt(2)–P(4)	171.8(3)	P(102)–Pt(4)–P(104)	172.1(3)
Hg(1)–Pt(2)–C(2)	117.5(9)	Hg(2)–Pt(4)–C(102)	122.3(8)
P(2)–Pt(2)–C(2)	87.1(8)	P(2)–Pt(4)–C(102)	87.8(8)
Pt(1)–Pt(2)–Hg(1)	59.2(1)	Pt(3)–Pt(4)–Hg(2)	58.3(1)
P(3)–Pt(1)–C(1)	86.2(7)	P(103)–Pt(3)–C(101)	83.6(10)
Pt(2)–Pt(1)–I(2)	60.7(1)	Pt(3)–Pt(4)–I(102)	61.2(1)
Pt(2)–Pt(1)–P(1)	94.0(2)	Pt(4)–Pt(3)–P(101)	92.8(2)
I(2)–Pt(1)–P(1)	93.7(2)	I(102)–Pt(3)–P(101)	91.9(2)
Hg(1)–Pt(1)–P(3)	86.5(2)	Hg(2)–Pt(3)–P(103)	92.0(2)
P(1)–Pt(1)–P(3)	172.0(3)	Pt(101)–Pt(3)–P(103)	172.2(3)
Hg(1)–Pt(1)–C(1)	124.6(8)	Hg(2)–Pt(3)–C(101)	115.3(10)
P(1)–Pt(1)–C(1)	88.2(7)	P(101)–Pt(3)–C(101)	89.2(10)
Pt(1)–Pt(2)–I(2)	61.4(1)	Pt(3)–Pt(4)–I(102)	61.2(1)
Pt(1)–Pt(2)–P(2)	93.6(2)	Pt(3)–Pt(4)–P(102)	94.3(2)
Hg(1)–Pt(2)–P(2)	93.0(2)	Hg(2)–Pt(4)–P(102)	92.5(2)
Pt(1)–Pt(2)–P(4)	94.5(2)	Pt(3)–Pt(4)–P(104)	91.8(2)
Pt(1)–Pt(2)–C(2)	177.8(8)	Pt(3)–Pt(4)–C(102)	92.5(2)
I(2)–Pt(2)–C(2)	121.9(9)	I(102)–Pt(4)–C(102)	118.1(8)
Pt(1)–Pt(2)–C(2)	176.6(10)	Pt(3)–Pt(4)–C(102)	177.8(8)
I(2)–Pt(2)–C(2)	121.9(9)	I(102)–Pt(4)–C(102)	118.1(9)
P(4)–Pt(2)–C(2)	84.7(8)	P(104)–Pt(4)–C(102)	86.1(8)

The structure of **4** is best understood by comparison to the d^9–d^9 A-frame $Pt_2(\mu\text{-HgCl}_2)(\mu\text{-dpm})_2Cl_2$, **2**.[8] In most A-frames, a slight twist is observed in the P–M–P vectors. In **2**, this twist is unusually large, as reflected in the torsional angles, 23.8 and 19.7°. This large twist has been shown by Hoffman and Hoffman to be determined by steric factors rather than electronic

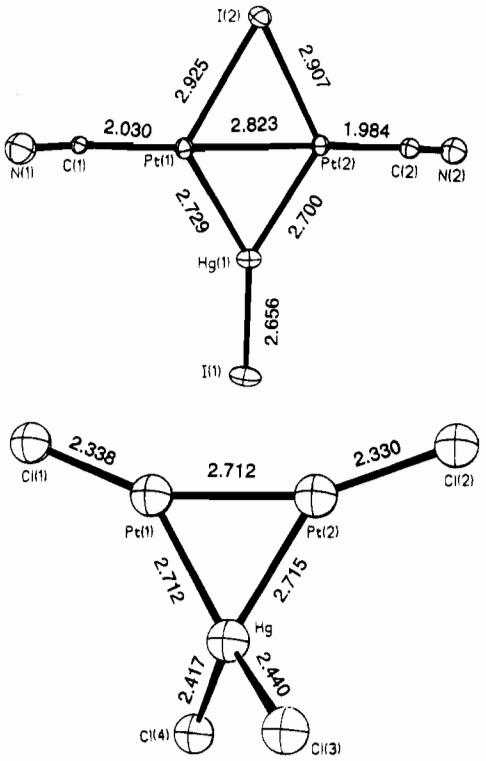

Figure 3. Comparison of the inner cores of $Pt_2(\mu\text{-I})(\mu\text{-HgI})(\mu\text{-dpm})_2(CN)_2$ (**4**), and $Pt_2(\mu\text{-HgCl}_2)(\mu\text{-dpm})_2Cl_2$ (**2**).

effects.[5] The steric interactions between the phenyl moieties and the chlorides on mercury are believed to cause the distorted geometry. In complex **4**, the steric interaction with the iodide on mercury is significantly reduced due to the planarity of the $(\mu\text{-I})Pt_2(\mu\text{-HgI})$ core; I(1) is elevated only 2.6° from the Pt_2Hg plane. A comparison of the cores of **2** and **4** shown in Figure 3 emphasizes the different geometries about the mercury fragments in the two complexes. The planarity of the platinum–mercury core results in very little distortion in the P–Pt–P vectors. Thus, the torsional angles P(1)–Pt(1)–Pt(2)–P(3), 1.4°, and P(2)–Pt(2)–Pt(1)–P(4), 3.0°, are very small. The small P–Pt–P twist may be related to the significantly larger Pt–Pt distance found in **4** (2.823(2) Å) as compared to the 2.7119(8) Å Pt–Pt bond length found in **2**.

Compared to the case of other A-frame complexes which contain a metal–metal bond, the presence of the bridging groups does not greatly disturb the $Pt_2(\mu\text{-dpm})_2(CN)_2$ core. The Pt(1)–Pt(2) bond is retained although elongated and the terminal cyanides remain relatively linear (Pt(2)–Pt(1)–C(1) 176.5(8)° (174.2(10)°) and Pt(1)–Pt(2)–C(2) 176.6(10)° (177.7(8)°). The distances and angles in the dpm ligands are unexceptional. The dpm ligands form a pseudo-six-membered ring with the platinum atoms and adopt the usual boat configuration with the methylene carbons directed toward the bridging iodide ligand. The Pt–P and Pt–C distances are in the range observed for other trans dpm structures.

Ignoring the Pt–Pt bond, the local geometry around each platinum atom best approximates a trigonal bipyramid. The bond angles of Hg–Pt–C 124.6(8)° (115.3(10)°) and 117.5(9)° (122.3(8)°), I–Pt–C 116.4(8)° (124.5(10)°) and 121.9(9)° (118.1(9)°), and Hg–Pt–I 120.50° (119.4(1)°) and 118.9(1)° (120.1(1)°) are close to the expected value of 120°. This feature is unlike other doubly bridged A-frames which show significant bending of the terminal ligands resulting in a less symmetrical placement of the equatorial ligands. In the doubly bridged rhodium A-frame, $Rh_2(\mu\text{-Cl})(\mu\text{-CO})(CO)_2(\mu\text{-dpm})_2$, this distortion is manifest in the following equatorial bond angles: C–Rh–$C_{terminal}$ (110.4 and 118.6°), Cl–Rh–$C_{terminal}$ (146.0 and 138.8°), and Cl–Rh–C (103.6° and 102.6°).[16]

Table 4. Atomic Coordinates ($\times 10^4$) and Equivalent Isotropic Displacement Coefficients ($Å^2 \times 10^3$) for $(NC)_2Pt_2(\mu\text{-AuCl})(\mu\text{-dpm})_2{\cdot}CH_2Cl_2$ (**6**)

	x	*y*	*z*	U^a
Pt(1)	6412(6)	38339(6)	707	196(4)
Pt(2)	−369(6)	28825(6)	−2707(14)	197(4)
Au	10859(7)	33187(6)	−8335(12)	253(5)
P(1)	259(4)	4651(4)	−127(6)	21(3)
P(2)	1126(4)	3061(4)	1640(6)	22(3)
P(3)	−600(4)	3666(4)	−938(6)	21(3)
P(4)	545(4)	2054(4)	451(6)	20(3)
Cl(1)	1990(5)	3326(6)	−1676(8)	57(4)
N(1)	871(16)	4673(15)	2533(22)	40(8)
N(2)	−1239(16)	2018(15)	−353(22)	42(8)
C(1)	758(16)	4380(16)	1826(22)	24(8)
C(2)	−784(18)	2315(17)	−301(26)	33(9)
C(15)	−119(15)	4385(15)	−1169(21)	18(7)
C(40)	1265(14)	2289(14)	1011(19)	14(7)

[a] Equivalent isotropic *U* defined as one-third of the trace of the orthogonalized U_{ij} tensor. Phenyl carbons and atoms of solvate molecules are omitted; see supplementary material.

Structure of $(NC)_2Pt_2(\mu\text{-AuCl})(\mu\text{-dpm})_2{\cdot}CH_2Cl_2$, 6. This compound crystallizes with one molecule of the complex and a molecule of dichloromethane in the asymmetric unit. There are no unusual contacts between these units. Atomic coordinates are given in Table 4, and selected interatomic distances and angles are given in Table 5. The molecular structure of **6** is shown in Figure 4. It consists of two Pt(CN) groups spanned by two mutually trans dpm ligands and bridged symmetrically by a AuCl fragment to form an A-frame. The Pt–Pt distance (2.821(2) Å) and the Pt–Au distances (2.633(2) and 2.648(2) Å) are consistent with the presence of a two-electron, three-center bond between the metals. The Pt–Pt bond completes the 16-electron count around each of the platinum atoms but places the metals in a highly distorted trigonal bipyramidal environment: Pt(2)–Pt(1)–Au 58.0(1)°, Pt(2)–Pt(1)–C(1) 150.5(10)°, Au–Pt(1)–C(1) 150.7(10)°; Pt(1)–Pt(2)–Au 57.5(1)°, Pt(1)–Pt(2)–C(2) 147.0(11)°, Au–Pt(2)–C(2) 155.3(11)°. The Pt_2Au cluster can be distinguished from the essentially undistorted d^8–d^8 A-frames $[Pt_2Cl_2(\mu\text{-Y})(\mu\text{-dpm})_2]^+$ (Y = SO_2, CH_2, CO), in which the coordination geometry of the metal centers is square planar and the Cl–Pt–Y angles are close to 180°.[17] This type of A-frame is not electron deficient and does not require a formal Pt–Pt bond to obtain a 16-electron count. The distortions in **6** can be compared to other electron deficient A-frames that contain a two-electron, three-center bond. This group is composed of a wide variety of species containing either small molecules or metal fragments at the apex. For example, in the d^7–d^7 complex $Rh_2Cl_2(\mu\text{-SO}_2)(\mu\text{-dpm})_2$, the metal atoms form a Rh–Rh bond with a distance of 2.78 Å and are characterized by S–Rh–Cl angles that are substantially decreased from 180°.[18]

Complex **6** is closely related to $Pt_2(\mu\text{-AuI})(\mu\text{-dpm})_2(CCBu^t)_2$.[19] Figure 5 shows the core of the molecular structures of **6** and $Pt_2(\mu\text{-AuI})(\mu\text{-dpm})_2(CCBu^t)_2$, **7**, for comparison. Table 5 compares important bond distances and angles of **6** and **7** and

(16) Cowie, M.; Mague, J. T.; Sanger, A. R. *J. Am. Chem. Soc.* **1978**, *100*, 3628. Cowie, M. *Inorg. Chem.* **1979**, *18*, 286. Olmstead, M. M.; Lindsay, C. H.; Benner, L. S.; Balch, A. L. *J. Organomet. Chem.* **1979**, *179*, 289.
(17) Azam, K. A.; Frew, A. A.; Lloyd, B. R.; Manojlovíc-Muir, Lj.; Muir, K. W.; Puddephatt, R. J. *Organometallics* **1985**, *4*, 1400.
(18) Cowie, M.; Dwight, S. K. *Inorg. Chem.* **1980**, *19*, 209.
(19) Manojlovíc-Muir, Lj.; Muir, K. W.; Treurnicht, I.; Puddephatt, R. J. *Inorg. Chem.* **1987**, *26*, 2418.

Table 5. Comparison of Bond Lengths (Å) and Angles (deg) for $(NC)_2(\mu\text{-AuCl})(\mu\text{-dpm})_2$ and $Pt_2(\mu\text{-AuI})(\mu\text{-dpm})_2(CCBu^t)_2$

Bond Lengths

$Pt_2(\mu\text{-AuCl})(\mu\text{-dpm})_2(CN)_2$		$Pt_2(\mu\text{-AuI})(\mu\text{-dpm})_2(CCBu^t)_2$[a]	
Pt(1)−Pt(2)	2.821(2)	Pt(1)−Pt(2)	2.837(1)
Pt(1)−Au	2.633(2)	Pt(1)−Au	2.656(2)
Pt(2)−Au	2.648(2)	Pt(2)−Au	2.661(2)
Pt(1)−C(1)	1.989(32)	Pt(1)−C(1)	2.01(3)
Pt(2)−C(2)	1.964(37)	Pt(2)−C(2)	2.02(3)
Pt(1)−P(1)	2.237(9)	Pt(1)−P(1)	2.283(6)
Pt(1)−P(2)	2.334(9)	Pt(1)−P(2)	2.279(5)
Pt(2)−P(3)	2.237(9)	Pt(2)−P(3)	2.274(5)
Pt(2)−P(4)	2.359(9)	Pt(2)−P(4)	2.289(6)
Au−Cl(1)	2.247(11)		

Bond Angles

$Pt_2(\mu\text{-AuCl})(\mu\text{-dpm})_2(CN)_2$		$Pt_2(\mu\text{-AuI})(\mu\text{-dpm})_2(CCBu^t)_2$[a]	
Au−Pt(1)−C(1)	150.7(10)	Au−Pt(1)−C(1)	151.0(7)
Au−Pt(2)−C(2)	155.3(11)	Au−Pt(2)−C(2)	151.7(6)
Pt(2)−Pt(1)−Au	58.0(1)	Pt(2)−Pt(1)−Au	57.8(1)
Pt(1)−Au−Pt(2)	64.6(1)	Pt(1)−Au−Pt(2)	64.5(1)
Pt(1)−Pt(2)−Au	57.5(1)	Pt(1)−Pt(2)−Au	57.7(1)
Au−Pt(1)−P(1)	89.4(2)	Au−Pt(1)−P(1)	88.8(2)
Au−Pt(1)−P(2)	92.6(2)	Au−Pt(1)−P(2)	94.5(2)
Au−Pt(2)−P(3)	94.8(2)	Au−Pt(2)−P(3)	93.3(2)
Au−Pt(2)−P(4)	86.0(2)	Au−Pt(2)−P(4)	88.4(2)
Pt(2)−Pt(1)−P(1)	95.3(2)	Pt(2)−Pt(1)−P(1)	95.6(2)
Pt(2)−Pt(1)−P(2)	90.9(2)	Pt(2)−Pt(1)−P(2)	87.5(2)
Pt(1)−Pt(2)−P(3)	87.8(2)	Pt(1)−Pt(2)−P(3)	86.8(2)
Pt(1)−Pt(2)−P(4)	92.3(2)	Pt(1)−Pt(2)−P(4)	92.3(6)
P(1)−Pt(1)−C(1)	92.2(10)	P(1)−Pt(1)−C(1)	90.2(7)
P(2)−Pt(1)−C(1)	83.1(10)	P(2)−Pt(1)−C(1)	86.1(6)
P(3)−Pt(2)−C(2)	90.8(11)	P(3)−Pt(2)−C(2)	85.3(6)
P(4)−Pt(2)−C(2)	88.7(11)	P(4)−Pt(2)−C(2)	92.3(6)
P(1)−Pt(1)−P(2)	173.6(3)	P(1)−Pt(1)−P(2)	176.3(3)
P(3)−Pt(2)−P(4)	179.1(3)	P(3)−Pt(2)−P(4)	177.6(3)
Pt(2)−Au−Cl(1)	156.1(3)	Pt(1)−Au−Cl(1)	147.5(2)
Pt(1)−Au−Cl(1)	138.5(3)	Pt(2)−Au−Cl(1)	148.1(2)

[a] Data taken from ref 19.

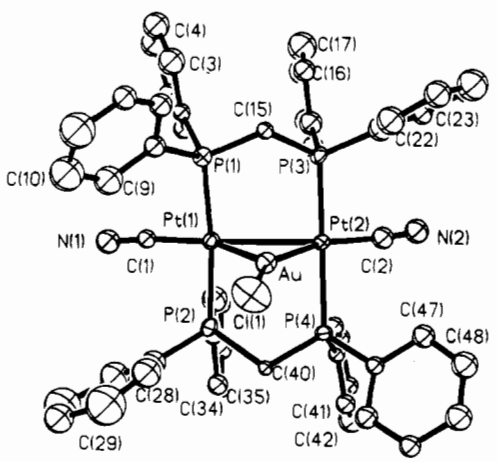

Figure 4. Perspective view of $Pt_2(\mu\text{-AuCl})(\mu\text{-dpm})_2(CN)_2$ with 50% thermal contours.

demonstrates that the bond angles about the platinum atoms are distorted from the idealized square planar geometry. In both complexes, the Au−Pt−C angles are substantially decreased from 180° (Au−Pt−C 150.7(10), 151.7(6)° for **6**, 151.0(7), 151.7(6)° for **7**) and the Pt−Pt separation (2.821(2) Å for **6**, 2.837(1) Å for **7**) and Pt−Au separation (2.648(2), 2.633(2) Å for **6**, 2.656(2) 2.661(2) Å for **7**) are consistent with metal−metal bonding.

The distances and angles in the dpm ligands are unexceptional. The Pt−P distances (2.237(9)−2.359(9) Å) are comparable with those usually observed in other trans-dpm structures. The Pt−C distances (1.989(32), 1.964(37) Å) are indicative of σ covalent bonding, and the C−N distances (1.211(45), 1.139(49) Å) are consistent with retention of the carbon−nitrogen triple bond. The Au−Cl(1) distance 2.247(11) Å falls within the expected range observed for other gold−chloride systems.

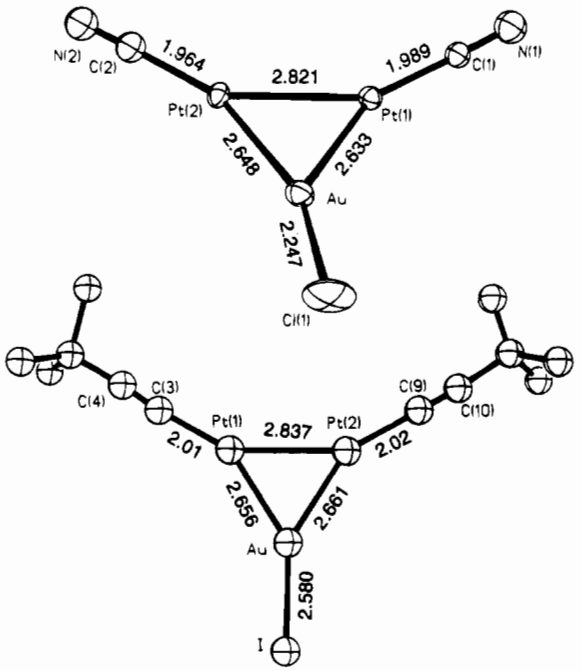

Figure 5. A comparison of the inner cores of $Pt_2(\mu\text{-AuCl})(\mu\text{-dpm})_2(CN)_2$ and $Pt_2(\mu\text{-AuI})(\mu\text{-dpm})_2(CCBu^t)$. Data for the latter come from ref 19.

Discussion

Previous studies showed that the Pt−Pt bond in $Pt_2(\mu\text{-dpm})_2Cl_2$ is highly reactive toward metal fragments. When a π-acceptor cyanide ligand is substituted for the π-donor chloride ligand, to give the compound $Pt_2(\mu\text{-dpm})_2(CN)_2$, there appears to be altered reactivity at the metal−metal bond, as indicated by the formation of the doubly bridging species $(NC)_2Pt_2(\mu\text{-I})(\mu\text{-HgI})(\mu\text{-dpm})_2$. In this trimetallic cluster, formation of the Pt−Hg bond and retention of the Pt−Pt bond results in a three-centered, two-electron bond utilizing predominantly a_1 orbitals. In this manner it resembles other electron deficient A-frames such as the complex $Pt_2(\mu\text{-HgCl}_2)(\mu\text{-dpm})_2Cl_2$.[8]

With the inclusion of the bridging iodide, the platinum atoms formally attain an 18-electron configuration while the mercury atom attains a 14-electron count. In contrast, in the A-frame cluster $Pt_2(\mu\text{-HgCl}_2)(\mu\text{-dpm})_2Cl_2$, the platinum atoms retain their 16-electron count and the mercury atom also attains a 16-electron count. Comparison of the electronic absorption spectra of $(NC)_2Pt_2(\mu\text{-I})(\mu\text{-HgI})(\mu\text{-dpm})_2$ and $Pt_2(\mu\text{-HgCl}_2)(\mu\text{-dpm})_2Cl_2$ shows that there is a significant difference in their electronic structures, as seen in Figure 1. For $(NC)_2Pt_2(\mu\text{-I})(\mu\text{-HgI})(\mu\text{-dpm})_2$ the spectrum is dominated by an intense band at 400 nm, while in $Pt_2(\mu\text{-HgCl}_2)(\mu\text{-dpm})_2Cl_2$, three absorption bands, located at 382, 428, and 480 nm, dominate the spectra. In addition, the former shows no luminescent behavior at room temperature or at 77 K, while the latter displays an intense, red emission at 677 nm.

The reaction of $Pt_2(\mu\text{-dpm})_2(CN)_2$ with Me_2SAuCl leads to the more conventional, singly bridged A-frame $Pt_2(\mu\text{-AuCl})(\mu\text{-dpm})_2(CN)_2$. In this complex platinum−platinum bonding is required to produce a 16-electron count at the platinum atoms. This bonding is consistent with the 2.821(2) Å platinum−

platinum distance. This produces a two-electron, three-center bond formed by the overlap of the a_1 orbital of the dimer and the a_1 orbital of the AuCl fragment. This allows the gold atom to attain a 14-electron configuration. Similarly, the cationic A-frame $[Pt_2Me_2(\mu\text{-H})(\mu\text{-dpm})_2]^+$, in which the apex bridging ligand, H^+, is isolobal with AuX, is thought to contain a three-centered, two-electron $Pt_2(\mu\text{-H})^+$ group, although the Pt−Pt distance is significantly longer (2.932(1) Å).[20] In contrast, the homonuclear trimetallic A-frame $[Pt_2(CNR)_2(\mu\text{-Pt}(CNR)_2)(\mu\text{-dpm})_2]^{2+}$ (R = 2,6-$Me_2C_6H_3$), which contains a ML_2 fragment that is isolobal with CH_2, does not require a metal−metal bond to attain a 16-electron configuration at the platinum atoms, nor is it indicated by the Pt−Pt bond distance of 3.304(2) Å.[21]

Experimental Section

Preparation of Compounds. Published methods were used to prepare the compounds $Pt_2(\mu\text{-dpm})_2Br_2$, $Pt_2(\mu\text{-dpm})_2Cl_2$,[22] and Me_2SAuCl.[23] The new compounds described here are stable to moisture and dioxygen and can be prepared without recourse to inert-atmosphere techniques.

$Pt_2(\mu\text{-dpm})_2(CN)_2$. To 116 mg (0.094 mmol) of $Pt_2(\mu\text{-dpm})_2Cl_2$ dissolved in 25 mL of dichloromethane was added 9 mg (0.184 mmol) of sodium cyanide dissolved in 20 mL of methanol. Upon addition, the yellow solution faded to cloudy green-yellow. After 1 h of stirring, the solution was filtered over Celite, and the volume was reduced to precipitate a lime-yellow solid; 77 mg (67%). This compound can be recrystallized from dichloromethane/methanol, but due to its low solubility and the lack of impurities, recrystallization was not performed. IR (Nujol mull): ν_{CN} 2098 cm^{-1}.

$(NC)_2Pt_2(\mu\text{-HgI})(\mu\text{-I})(\mu\text{-dpm})_2$, 4. To 72 mg (0.059 mmol) of $Pt_2(\mu\text{-dpm})_2(CN)_2$ dissolved in 25 mL of dichloromethane was added 27 mg (0.059 mmol) of HgI_2 dissolved in methanol. Upon addition, the yellow solution turned orange. After 1 h of stirring, the volume was reduced to 10 mL to yield a yellow-orange crystalline powder; 79 mg (80%). This compound can be recrystallized from dichloromethane/diethyl ether. IR (Nujol mull): ν_{CN} 2127 cm^{-1}.

$(NC)_2Pt_2(\mu\text{-HgBr})(\mu\text{-Br})(\mu\text{-dpm})_2$, 5. To 77 mg (0.063 mmol) of $Pt_2(\mu\text{-dpm})_2(CN)_2$ dissolved in 25 mL of dichloromethane was added 25 mg (0.069 mmol) of $HgBr_2$ dissolved in methanol. Upon addition, the yellow solution turned bright yellow. After 1 h of stirring, the volume was reduced to 10 mL to yield a yellow crystalline powder; 67 mg (85%). This compound can be recrystallized from dichloromethane/diethyl ether. IR (Nujol mull): ν_{CN} 2126 cm^{-1}.

$(NC)_2Pt_2(\mu\text{-AuCl})(\mu\text{-dpm})_2$, 6. To 60 mg (0.050 mmol) of $Pt_2(\mu\text{-dpm})_2(CN)_2$ dissolved in 25 mL of dichloromethane was added 14 mg (0.048 mmol) of Me_2SAuCl. Upon addition, the pale yellow solution turned a darker yellow. After 1 h of stirring, the volume was reduced and methanol was added to crystallize a bright yellow-green solid; 30 mg (42%). This compound can be recrystallized from dichloromethane/diethyl ether. IR (Nujol mull): ν_{CN} 2120 cm^{-1}.

Physical Measurements. ^{31}P NMR Spectroscopy. The $^{31}P\{^1H\}$ NMR spectra were recorded with proton decoupling on a General Electric QE-300 NMR spectrometer that operates at 121.7 MHz with an external 85% phosphoric acid standard and the high field positive convention for reporting chemical shifts.

^{195}Pt NMR Spectroscopy. The ^{195}Pt NMR spectrum was recorded with proton decoupling on a General Electric QE-300 NMR spectrometer that operates at 64.3 MHz. All data points were accumulated over a 10 kHz spectral window. The delay between each acquisition pulse was set at 500 ms, and a 12 μs (90°) pulse was used to acquire data. H_2PtCl_6 in D_2O was used as an external reference.

Infrared and Electronic Spectroscopy. Infrared spectra were recorded from Nujol mulls using an IBM IR 32 infrared spectrometer.

Table 6. Crystal Data and Data Collection and Structure Solution Parameters for $Pt_2(\mu\text{-HgI})(\mu\text{-I})(\mu\text{dpm})_2(CN)_2\cdot CH_2Cl_2\cdot 1.5H_2O$ (**4**) and $Pt_2(\mu\text{-AuCl})(\mu\text{-dpm}_2)_2(CN)_2\cdot CH_2Cl_2$ (**6**)

	4	**6**
formula	$C_{53}H_{41.5}I_2N_2P_4Pt_2HgCl_2O_{1.5}$	$C_{53}H_{44}N_2P_4Pt_2AuCl_2$
fw	1770.2	1490.8
color and habit	orange parallelepipeds	yellow parallelepipeds
crystal system	triclinic	tetragonal
space group	$P\bar{1}$	$P4_3$
a, Å	15.311(3)	20.933(5)
b, Å	16.132(5)	
c, Å	24.911(6)	14.381(6)
α, deg	82.99(2)	
β, deg	81.02(2)	
γ, deg	89.80(2)	
V, Å^3	6031(3)	6302(4)
T, K	130	130
Z	4	4
d_{calcd}, g cm^{-3}	1.950	1.571
radiation (λ, Å)	Mo Kα (0.710 73)	Mo Kα (0.710 73)
μ(Mo Kα), cm^{-1}	84.2	69.68
range of transm factors	0.65−0.97	0.61−0.99
no. of data collected	15 892	6130
no. of unique data	15 892	4378
no. of data refined	11 040 ($F > 4.0\sigma(F)$)	3473 ($F > 4.0\sigma(F)$)
no. of params refined	416	300
R^a	0.0842	0.0592
$R_w{}^b$	0.1172 ($w = 1/\sigma^2(F_o)$)	0.0810 ($w = 1/\sigma^2(F_o)$)

$^a R = \sum||F_o| - |F_c||/|F_o|$. $R_w = \sum||F_o| - |F_c||w^{1/2}/\sum|F_o|w^{1/2}$.

Electronic spectra were recorded with a Hewlett-Packard 8450A spectrophotometer in dichloromethane.

X-ray Data Collection for $(NC)_2Pt_2(\mu\text{-HgI})(\mu\text{-I})(\mu\text{-dpm})_2\cdot CH_2Cl_2\cdot 1.5H_2O$, 4. Orange parallelepipeds of the complex were obtained by diffusion of diethyl ether into a dichloromethane solution of the complex. These were coated with a light hydrocarbon oil, mounted on a glass fiber with silicone grease, and placed in the 130 K nitrogen stream of a Siemens R3m/V diffractometer that was equipped with a locally modified Enraf-Nonius low-temperature apparatus. Unit cell parameters were determined by least-squares refinement of 28 reflections with 16° < 2θ < 20°. Two check reflections showed only random (<1%) fluctuation in intensity during data collection. The data were corrected for Lorentz and polarization effects. Crystal data are given in Table 6. Scattering factors and corrections for anomalous dispersion were taken from a standard source.[24]

Solution and Structure Refinement for $(NC)_2Pt_2(\mu\text{-HgI})(\mu\text{-I})(\mu\text{-dpm})_2\cdot 2CH_2Cl_2\cdot 1.5H_2O$, 4. Calculations were performed using the Siemens SHELTX PLUS system of programs. The structure refinement was hampered by unusually large absorptions by the platinum and mercury atoms. The structure was solved by direct methods. There are two complete molecules in the asymmetric unit and four molecules of dichloromethane which were modeled at half-occupancy. The phenyl rings on the dpm ligands were fixed as rigid bodies. Hydrogen atoms were included in the refinement model. Their positions were calculated by the use of a riding model with a C−H distance fixed at 0.96 Å and a thermal parameter of $U = 0.035$ Å. Hydrogen atoms were not added to phenyl ring C(28)−C(33) due to the large amount of disorder. The disorder was modeled as two phenyl rings with the carbons at half-occupancy in each ring. Only the Pt, Hg, I, and P atoms were allowed to refine anisotropically. An absorption correction was applied.[25] Three peaks with electron density ca. 3 e/Å^{-3} were modeled as oxygen atoms at half-occupancy: they were presumed to be water molecules. Their thermal parameters were fixed at $U = 0.040$. The final difference map contained five peaks with electron density ≈3.2 e/Å^{-3}. Peaks Q(2),

(20) Brown, M. P.; Cooper, S. J.; Frew, A. A.; Manojlovíc-Muir, Lj.; Muir, K. W.; Puddephatt, R. J.; Thomson, M. A. *J. Chem. Soc., Dalton Trans.* **1982**, 299.
(21) Yamamoto, Y.; Takahashi, K.; Yamazaki, H. *J. Am. Chem. Soc.* **1986**, *108*, 2458.
(22) Brown, M. D.; Puddephatt, R. J.; Rashidi, M.; Seddon, D. K. *J. Chem. Soc., Dalton Trans.* **1977**, 951.
(23) Ray, P. C.; Sen, S. C. *J. Indian Chem. Soc.* **1930**, *7*, 67.
(24) *International Tables for X-ray Crtstallography*; Kynoch Press: Birmingham, England, 1974; Vol. 14.
(25) Program XABS. The method obtains an empirical absorption tensor from an expression relating F_o and F_c: Moezzi, B. Ph.D. Dissertation, University of California, Davis, 1987.

Q(3), and Q(4), with electron density = 3.10 e/Å^{-3}, were located near Pt(1), Hg(1), and Cl(1), respectively. Peak Q(1) was located 1.52 Å from Q(11) with electron density = 3.17 e/Å^3 and Q(5) had electron density = 3.05 e/Å^{-3}. Initial refinement was made without assigning these peaks. Later Q(1) and Q(11) were assigned as a methanol at half-occupancy and Q(5) as a water molecule at half-occupancy. Neither of these assignments had any effect on the overall structure, and the final R and R_w values remained the same. Therefore the final difference map did not contain these assignments and the largest peak in the final difference map remains Q(1) with a density of 3.17 e/Å^{-3} and is located 1.5 Å from Q(11). The goodness of fit was calculated at 1.305.

X-ray Data Collection for $(NC)_2Pt_2(\mu\text{-AuCl})(\mu\text{-dpm})_2\cdot CH_2Cl_2$, 6. Yellow-orange parallelepipeds of the complex were obtained by diffusion of diethyl ether into a dichloromethane solution of the complex. These were coated with a light hydrocarbon oil, mounted on a glass fiber with silicone grease, and placed in the 130 K nitrogen stream of a Siemens R3m/V diffractometer that was equipped with a locally modified Enraf-Nonius low-temperature apparatus. Unit cell parameters were determined by least-squares refinement of 35 reflections with $6° < 2\theta < 46°$. Two check reflections showed only random (<1%) fluctuation in intensity during data collection. The data were corrected for Lorentz and polarization effects. Crystal data are given in Table 6. Scattering factors and corrections for anomalous dispersion were taken from a standard source.[24]

Solution and Structure Refinement for $(NC)_2Pt_2(\mu\text{-AuCl})(\mu\text{-dpm})_2\cdot CH_2Cl_2$, 6. Calculations were performed using the Siemens SHELTX PLUS system of programs. The structure was solved by direct methods. Hydrogen atoms were included in the refinement model. Their positions were calculated by the use of a riding model with C−H distance fixed at 0.96 Å and a thermal parameter of U = 0.035 Å. Only Pt, Au, Cl, and P atoms were allowed to refine anisotropically. The Cl atoms on the dichloromethane molecules were kept isotropic. An absorption correction was applied.[25] The largest peak in the final difference map had a density of 1.52 e/Å^{-3} and was 0.62 Å from Cl(3).

Acknowledgment. We thank the National Science Foundation (Grants CHE9022909 and CHE-9321257) for support and Johnson Matthey, Inc., for a loan of platinum chloride.

Supplementary Material Available: Tables of crystallographic experimental details, atomic coordinates, bond distances, bond angles, anisotropic thermal parameters, and hydrogen atom positions for $(NC)_2Pt_2(\mu\text{-HgI})(\mu\text{-I})(\mu\text{-dpm})_2\cdot 2CH_2Cl_2\cdot 1.5H_2O$ and $(NC)_2Pt_2(\mu\text{-AuCl})(\mu\text{-dpm})_2\cdot CH_2Cl_2$ (21 pages). Ordering information is given on any current masthead page.